IJCRT.ORG ISSN : 2320-2882
INTERNATIONAL JOURNAL OF CREATIVE RESEARCH THOUGHTS (IJCRT)
An International Open Access, Peer-reviewed, Refereed Journal

THREE PORT DC-DC CONVERTER OPERATED SMART ELECTRIC VEHICLE(EV) CHARGING STATION USING STAND ALONE PHOTO VOLTAIC SYSTEM.

[1]SINHA RAVIRANJANKUMAR VINAYKUMAR, [2]SWAPNIL BHANUDAS PATIL, [3]NISHIT JOSHI, [4]RAHUL JADAV, [5]SHANU SHRIVASTAV
[1]STUDENT, [2]STUDENT, [3]STUDENT, [4]PROFESSOR, [5]STUDENT
[1]GUJARAT TECHNICAL UNIVERSITY,
[2]GUJARAT TECHNICAL UNIVERSITY,
[3]GUJARAT TECHNICAL UNIVERSITY,
[4]GUJARAT TECHNICAL UNIVERSITY,
[5]GUJARAT TECHNICAL UNIVERSITY

Abstract-Three-port dc to dc converter operated smart electric vehicle (EV) charging station using stand-Alone Photovoltaic system can be said as the first step taken in the direction of the Electric Vehicle area, in terms of the charging for the battery of the Vehicle. System efficiency and cost effectiveness are most importance for photovoltaic (PV)system. The theoretical analysis is conducted to analyze the operating modes followed by the MATLAB/SIMULATION and the analysis of the simulation results provides a clear platform for the hardware model for the converter. And that can be verified by the 10-Watt prototype model and by performing all the critical modes of operation with the hardware model the results can be achieved and which can be upto the mark with the simulation results. Therefore, it can be concluded that when grid is not available for the charging purpose of the EV the Stand-Alone PV system with the Three Port DC-DC converter can be a feasible solution. That can be said as the first milestone towards the new era of the EV and its frequent requirement of charging

Keywords – TP Converter, PV module, PWM strategy, Operational Modes.

I.Introducation

From the past few years there are so many evaluation came in the transportation vehicle and their demand is continuously increasing due to that fact the mankind are facing the problem of scarcity of fossil fuel therefore it is very much important to find it alternative so many research work done in this area from the past decade. Solar energy is a primary and renewable source of energy. As the cost of photovoltaic (PV) panels is seen to reduce continuously, PV-based power generation is gaining in popularity for both grid-connected and stand-alone systems. Stand-alone systems are independent of utility grids and commonly employed for satellites, space stations, unmanned aerial vehicles, and domestic applications. Such systems require storage elements to accommodate the intermittent generation of solar power, Over the years, research effort has been directed toward improving the power conversion efficiency as

well as the power density by weight and the power density by volume, Traditionally, the two-port topology utilizes the dual active bridges. and the half or full bridges can support the multiport structure to some extent. A combination of Flyback-Forward converter with full bridge has shown some advantages in zero voltage switching (ZVS) and high conversion ratio for fuel cell applications. A modified half-bridge converter is reported in, which consists of one PV input port, one bidirectional battery port, and an isolated output for satellite applications. However, in these converters, a multiinput-multi-output solution is generally difficult to achieve for power electronic applications. in multiple-input converters (e.g., three-port converters) can provide a single-unit solution interfacing multiple energy sources and common loads. They perform better than traditional two-port converters due to their lower part count and smaller converter size. In particular, the isolated three-port converter (ITPC) has become an attractive topology for various applications owing to their multiple energy source connection, compact structure, and low cost. In this topology, a simple power-flow management scheme can be used since the control function is centralized. A high-frequency transformer can provide galvanic isolation and flexible voltage conversion ratio. The ITPC is usually integrated into an individual converter such as forward, push–pull, full-bridge, and Flyback converters, The ITPC utilizes the triple active bridges (TAB) with inherent features of power controllability and ZVS. Their soft switching performance can be improved if two series-resonant tanks are implemented. An advanced modulation strategy is reported in, which incorporates a phase shift (PS) and a PWM to extend the operating range of ZVS. Nonetheless, the TAB topology suffers from the circuit complexity using three active full bridges or half bridges and the power loss caused by reactive power circulation. Therefore, a Buck-Boost converter is proposed to integrate a three-port topology in the half bridge and to decompose the multivariable control problem into a series of independent single-loop subsystems. By doing so, the power flow in each loop can be independently controlled. The system is suitable for PV-battery applications since one converter interfaces with the three components of the PV array, battery, and loads. However, in each energy transfer state, current passes through at least five inductor windings, especially under high-switching frequency conditions, giving rise to power loss; its peak efficiency is less than 90% and its power capability is limited by the transformer size. Based on these topologies, a new three-port dc–dc converter is developed in this paper to combine a new ITPC topology with an improved control strategy, and to achieve decoupled port, control, flexible power flow, and high-power capability while still making the system simple and cheap.

II. LITERATURE REVIEW

The proposed converter topology is illustrated in Fig. 1. The main switches S1 and S2 transfer the energy from the PV to the battery or load, and can work in either interleaved or synchronous mode. The switches S3 and S4 are operated in the inter leaved mode to transfer energy from source to load. L1 and L2 are two coupled inductors whose primary winding (n1) is employed as a filter and the secondary windings (n2) are connected in series to achieve a high-output voltage gain. LLK is the leakage inductance of the two coupled inductors and N is the turns ratio from n2/n1. CS1, CS2, CS3, and CS4 are the parasitic capacitors of the main switches S1, S2, S3, and S4, respectively.

There are three operational modes for the converter, in mode 1, the PV array supplies power to load and possibly also to the battery,

corresponding to the daytime operation of the PV system. Two 180° out-of-phase gate signals with the same duty ratio (D) are applied to S_1 and S_2, while S_3 and S_4 remain in a synchronous rectification state. When in the steady-state operation, there are four states in one switching period, of which the equivalent circuits are shown in Fig. 3. The steady-state waveforms of the four states are depicted in Fig. 4, where V_{GS1}, V_{GS}, V_{GS3}, and V_{GS4} are the gate drive signals; V_{ds1} and V_{ds2} are the voltage stresses of S_1 and S_2; i_{L1a} and i_{L2a} are the currents through L_{1a} and L_{2a}, respectively. I_b is the current through the battery, i_{s1} is the current through S_1, v_{Do1} is the voltage stress of the output diode D_{o1}, and i_{Do1} is the current through D_{o1}.

State 1 [t_0 –t_1]: The main switches S_1 and S_2 are both in turn- on state before t_0. The two coupled inductors work in the fly back state to store energy from the PV array. The output rectifier diodes D_{o1} and D_{o2} are both reverse-biased. The energy stored in the secondary output capacitors C_{o1} and C_{o2} transfers to the load.

State 2 [t_1 –t_2]: At t_1, S_2 turns OFF, S_4 turns ON, while the diodes D_{o1} is ON. The primary side of the coupled inductor L_2 charges the battery through S_4. During this state, L_1 operates in the forward mode and L_2 operates in the fly back mode to transfer energy to the load. When S_1 turns ON and S_2 turns OFF, the primary voltage of the coupled inductor L_1 is V_{pv} and the voltage on L_2 is $-V_B$.

State 3 [t_2 –t_3]: At t_2, S_2 turns ON, which forces the two coupled inductors work in the fly back state to store energy and D_{o2} is reverse-biased. The energy stored in C_{o1} and C_{o2} transfers to the load. At t_3, the leakage inductor current decreases to zero and the diode D_{o1} turns OFF.

State 4 [t_3 –t_4]: At t_3, S_1 turns OFF and S_3 turns ON, which turns D_{o2} ON. The primary side of coupled inductor L_1 charges the battery through S_3. During this state, L_2 operates in the forward mode and L_1 operates in the flyback mode to transfer energy to the load. When S_1 turns ON and D_{o2} turns OFF, a new switching period is started.

In mode 2, the battery supplies power to the load, as shown in Fig. 5(a), indicating the nighttime operation of the stand-alone system. The circuit works as the Flyback-Forward converter, where S_3 and S_4 are the main switches, C_c, S_1, and S_2 form an active clamp circuit. When the load is disconnected, the stand- alone system enters into mode 3. The PV array charges battery without energy transferred to the load due to the opposite series- connected structure of the coupled inductor [see Fig. 5(b)]. S_1 and S_2 work simultaneously and the topology is equivalent to two paralleled Buck-Boost converters.

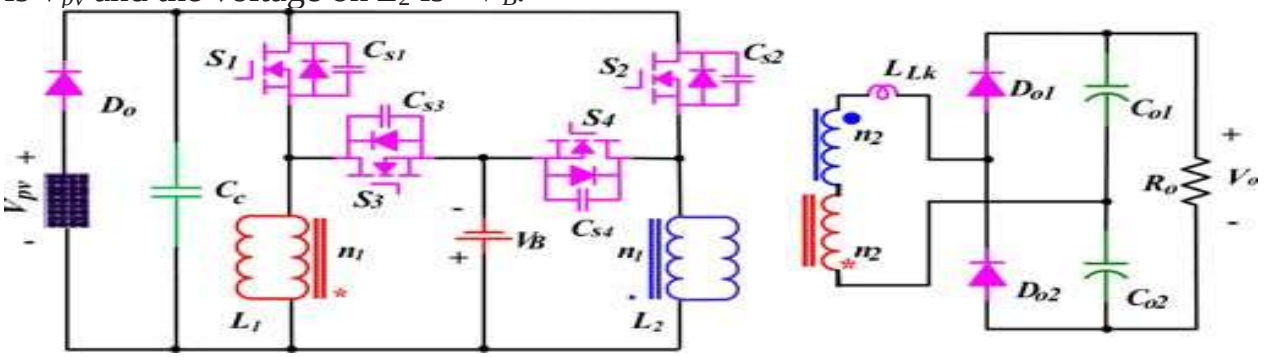

fig. 1. Proposed converter topology.

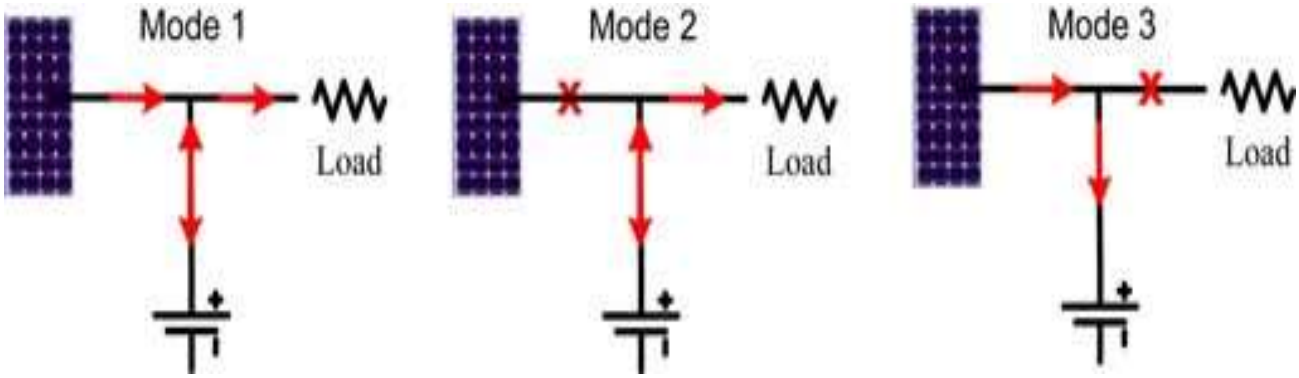

Fig. 2. Three operation modes of the proposed converter.

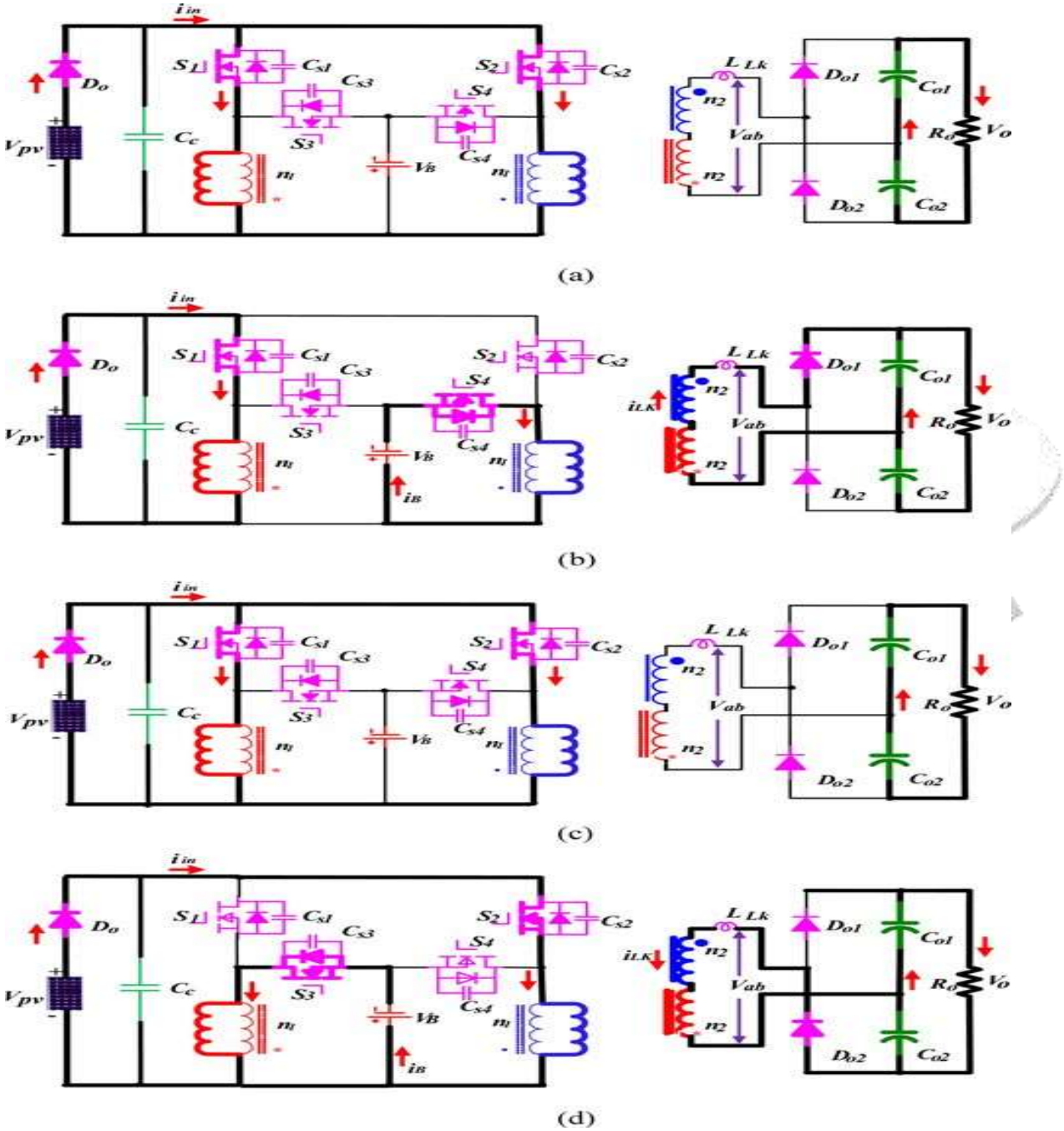

Fig. 3. Four operating states of the proposed converter in mode 1.

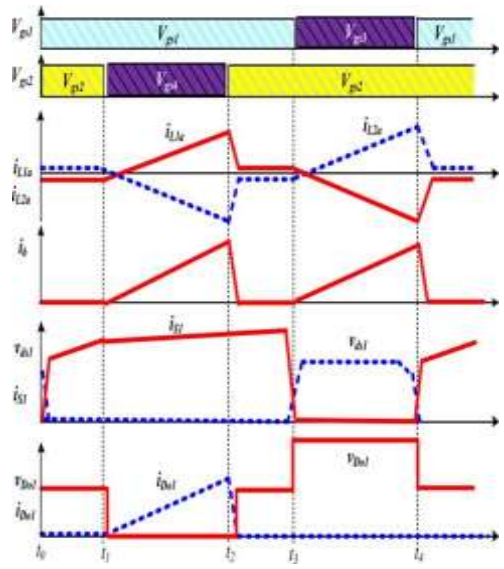

Fig. 4. Waveforms of the proposed converter under mode 1.

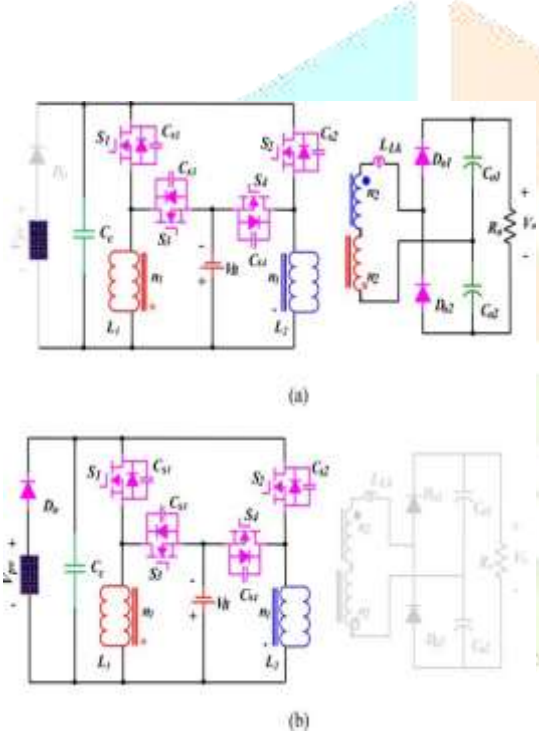

Fig 5. Converter operating 2 and 3 (a) mode2, (b) mode 3

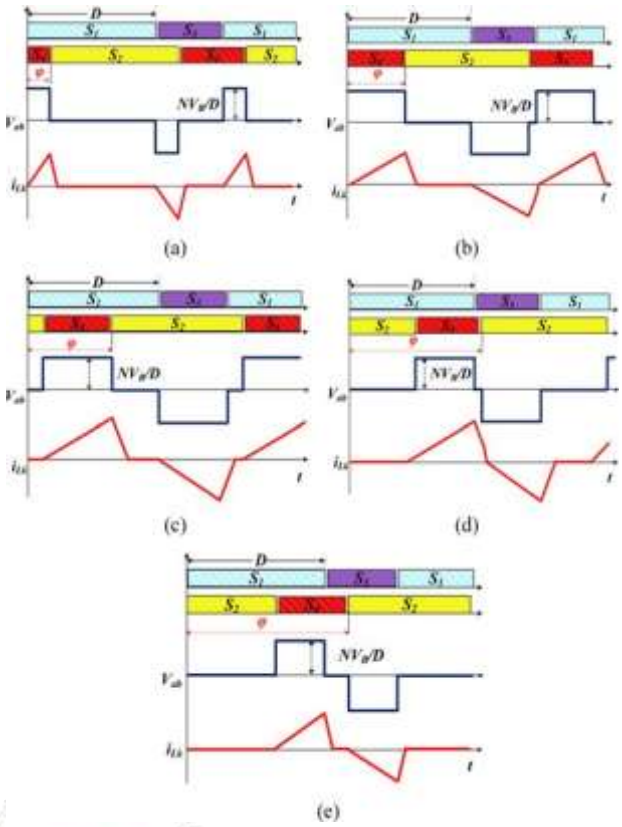

Fig 6. five operational cases for (a) case1, (b) case2, (c) case3, (d) case4, and (e) case5.

active clamp circuit. When the load is disconnected, the stand- alone system enters into mode 3. The PV array charges battery without energy transferred to the load due to the opposite series- connected structure of the coupled inductor [see Fig. 5(b)]. S_1 and S_2 work simultaneously and the topology is equivalent to two paralleled Buck-Boost converters.

A. SIMULATION TEST:

Simulation work is carried out in the PSIM environment to establish the relationship of the phase angle shift and output volt- age, and to test the proposed control scheme including MPPT and output voltage control. Fig. 7(a) and (b) shows the phase angle shift control and output voltage response at D>=0.5 and D<=0.5 conditions. The phase angle is divided into five portions in accordance with five cases in the theoretical analysis. In Fig. 11(a), the output voltage is controllable for cases 1, 2, 4, and 5 by the phase angle but it is not in case 3. When $D < 0.5$ [see Fig. 7(b)],

the relationship becomes more linear than Fig. 7(a). As shown in Fig. 7(c), the PV voltage is regulated to 12.8 V, which re resents the MPP. The output voltage is controlled at 80 V as expected. Fig. 7(d) presents waveforms of the gate signals and secondary-side inductance current. At 45ms, the load resistance is suddenly reduced from 100 to 40 Ω (perturbation); the output voltage drops to 73 V, and recovers to 80 V after 15ms adjustment, as presented in Fig. 7(e). It is also seen in Fig. 7(f) that the PV array voltage recovers to the MPPT voltage after 1ms adjustment when subjected to an input power step change from 500 to 1000 W/m^2 (perturbation) at 40ms.

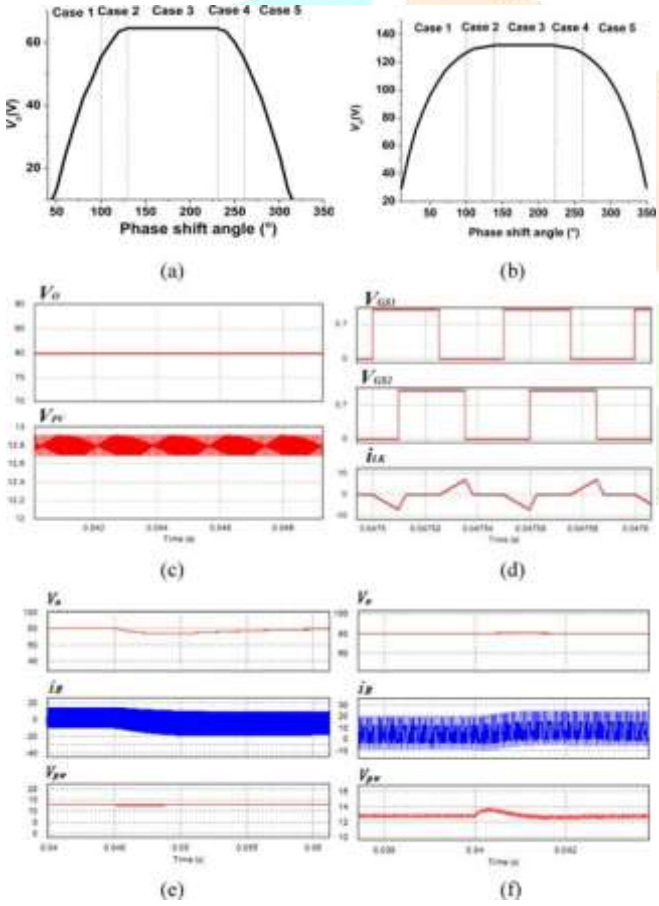

Fig 7. Simulation Results of the proposed control scheme (a) D>0.5 (D=0.66), (b)D<0.5 (D=0.33) (c) output and pv voltages (d) second side current of the output inductor (e)response to the load step, and (f) response to the power step

resents the MPP. The output voltage is controlled at 80 V as expected. Fig. 7(d) presents waveforms of the gate signals, and secondary-side inductance current. At 45ms, the load resistance is suddenly reduced from 100 to 40 Ω (perturbation); the output voltage drops to 73 V, and recovers to 80 V after 15ms adjustment, as presented in Fig. 7(e). It is also seen in Fig. 7(f) that the PV array voltage recovers to the MPP voltage after 1ms adjustment when subjected to an input power step change from 500 to 1000 W/m^2 (perturbation) at 40ms.

B. Experimental test

The proposed converter topology and control scheme are implemented in a 250-W prototype (see Fig. 12) with a Texas Instruments TMS320F28335 controller. Experimental tests are conducted with a PV array simulator (Agilent Technology E4360A) to obtain the steady-state waveforms of the proposed converter under different operating conditions.

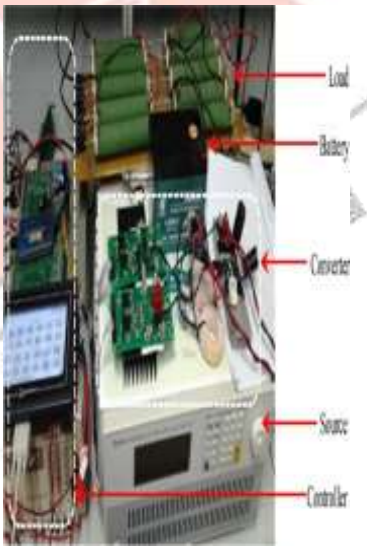

Fig 8. Experimental setup of the propsed converter test system.

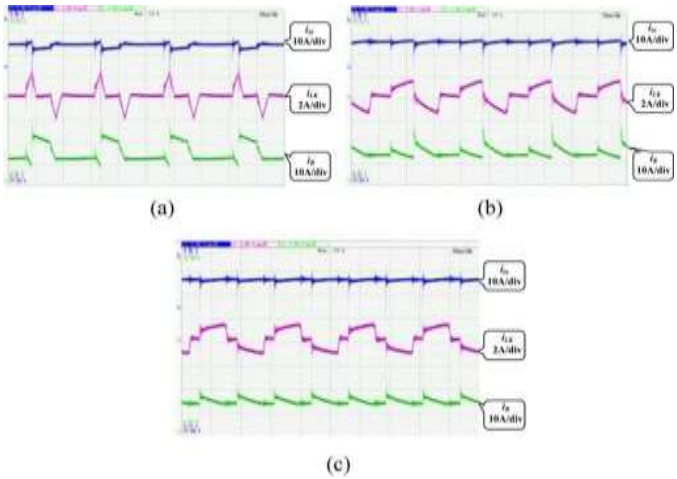

Fig 9. Current waveforms for different cases (D>0.5 mode 1), (a) case1 (phi=30), (b)case2 (phi=120), case3 (phi=180).

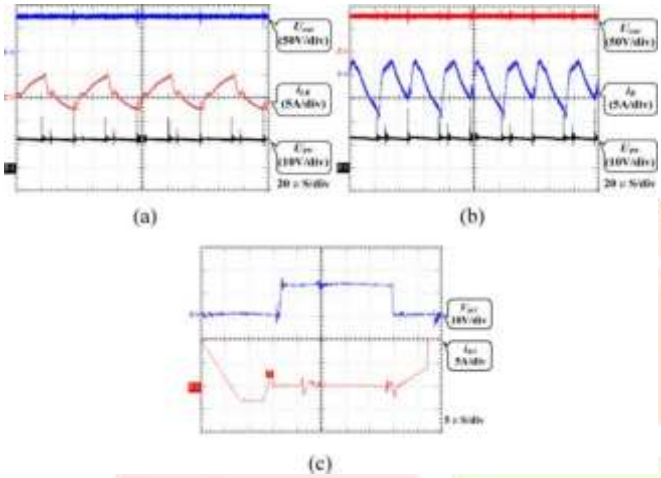

Fig 10. Experiment results of voltage regulation performance, (a) output voltage (b). PV voltage, and (c) s1 switching performance.

C. THREE PORT DC TO DC CONVERTER CIRCUIT DIAGRAM

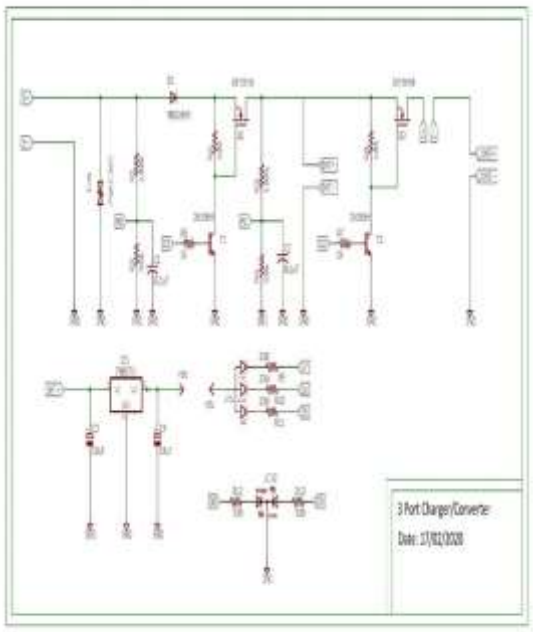

FIG 11. Three port dc to dc converter circuit diagram

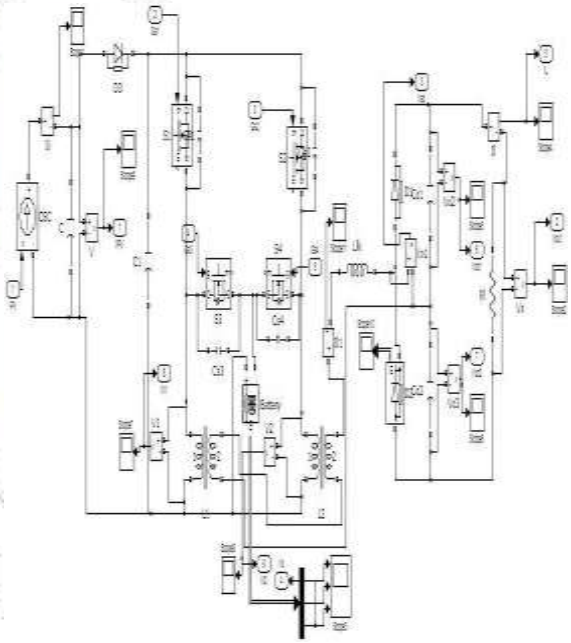

Fig 12. MATLAB/ SIMULATION MODEL OF CONVERTER

CONCLUSION

This paper has presented an isolated three-port dc–dc converter for stand-alone PV systems, based on an improved Flyback-Forward topology. The converter can provide a high step-up capability for power conversion systems including the PV array, the battery storage, and the isolated load consumption. Three operating modes are

analyzed and have shown the effective operation of the proposed topology for PV applications. From simulation and experimental tests, it can be seen that the output voltage and PV voltage can be controlled independently by the phase angle shift and PWM, respectively. The decoupled control approach is a simple but effective way to achieve the regulation of output voltage and PV voltage, which is important for MPPT of stand-alone PV systems. In addition, a 250-W converter is prototyped and tested to verify the effectiveness of the proposed converter topology and control scheme.

The developed technology is capable of achieving MPPT, high conversion ratio, and multiple operating modes, while still making the converter relatively simple, light, efficient, and cost- effective.

REFERENCES

[1] K. Shenai, P. G. Neudeck, and G. Schwarze, "Design and technology of compact high-power converters," *IEEE Aerosp. Electron. Syst. Mag.*, vol. 16, no. 3, pp. 27–31, Aug. 2001.

[2] H. Wu, P. Xu, H. Hu, Z. Zhou, and Y. Xing, "Multi-port converters based on integration of full-bridge and bidirectional DC-DC topologies for re-newable generation systems," *IEEE Trans. Ind. Electron.*, vol. 61, no. 2, pp. 856–869, Feb. 2014.

[3] R. J. Wai, C. Y. Lin, and Y. R. Chang, "High step-up bidirectional isolated converter with two input power sources," *IEEE Trans. Ind. Electron.*, vol. 56, no. 7, pp. 2629–2643, Jul. 2009.

[4}K. Basu and N. Mohan, "A high-frequency link single-stage PWM inverter with common-mode voltage suppression and source-based commutation of leakage energy," *IEEE Trans. Power Electron.*, vol. 28, no. 8, pp. 3907– 3918, Oct. 2014.

[5] C. Konstantopoulos and E. Koutroulis, "Global maximum power point tracking of flexible photovoltaic modules," *IEEE Trans. Power Electron.*, vol. 29, no. 6, pp. 2817–2828, Oct. 2014.

[6] W. Li, W. Li, X. Xiang, Y. Hu, and X. He, "High step-up interleaved converter with built-in transformer voltage multiplier cells for sustain- able energy applications," *IEEE Trans. Power Electron.*, vol. 29, no. 6, pp. 2829–2836, Jun. 2014.

[7] K. Shenai, P. G. Neudeck, and G. Schwarze, "Design and technology of compact high-power converters," *IEEE Aerosp. Electron. Syst. Mag.*, vol. 16, no. 3, pp. 27–31, Aug. 2001.

[8] H. Tao, J. L. Duarte, and M. A. M. Hendrix, "Three-port triple-half-bridge bidirectional converter with zero-voltage switching," *IEEE Trans. Power Electron.*, vol. 23, no. 2, pp. 782–792, Mar. 2008.

[9} H. Tao, A. Kotsopoulos, J. L. Duarte, and M. A. M. Hendrix, "Family of multiport bidirectional DC-DC converters," *Proc. IEE ElectriPower Appl.*, vol. 153, no. 3, pp. 451–458, May 2006.

[10] Z. Wang and H. Li, "An integrated three-port bidirectional DC-DC con- verter for PV application on a DC distribution system," *IEEE Trans. Power Electron.*, vol. 28, no. 10, pp. 4612–4624, Oct. 2013.

[11] H. Tao, A. Kotsopoulos, J. L. Duarte, and M. A. M. Hendrix, "Transformer- coupled multiport ZVS bidirectional DC-DC converter with wide input range," *IEEE Trans. Power Electron.*, vol. 23, no. 2, pp. 771–781, M

ar. 2008.


IJCRT